ISIJ International, Vol. 40 (2000), No. 9, pp. 902–908

Retained Austenite Characteristics and Tensile Properties in a TRIP Type Bainitic Sheet Steel

Koh-ichi SUGIMOTO, Tsutomu IIDA,[1)] Jyunya SAKAGUCHI[1)] and Takahiro KASHIMA[2)]

Department of Mechanical Systems Engineering, Shinshu University, Wakasato, Nagano 380-8553 Japan.
E-mail: sugimot@gipwc.shinshu-u.ac.jp. 1) Graduate School, Shinshu University, Wakasato, Nagano 380-8553 Japan.
2) Kakogawa Works, Kobe Steel Ltd., Onoe-cho, Kakogawa 675-0023 Japan.

(*Received on December 21, 1999; accepted in final form on May 15, 2000*)

Retained austenite characteristics and tensile properties in a 0.2C–1.5Si–1.5Mn, mass%, high-strength cold-rolled "TRIP type bainitic steel" which was associated with the transformation induced plasticity (TRIP) of the retained austenite were investigated. The steel mainly consisted of bainitic ferrite lath matrix, blocky martensites and stable retained austenite films of 5–12 vol%. When austempered at temperatures above M_S temperature, the steel possessed high tensile strength of 900 MPa, large total elongation of 15–20 % and large reduction of area of 40–60 %. The good ductility was mainly owing to uniform fine lath structure, initial martensite and the TRIP effect of retained austenite, as well as a small contribution of long range internal stress resulting from untransformed retained austenite films.

KEY WORDS: retained austenite; bainitic ferrite; ductility; high-strength steel; TRIP; heat-treatment; austempering.

1. Introduction

The transformation induced plasticity (TRIP)[1)] of retained austenite is very useful in improving the press formability of high-strength sheet steel. In fact, it was demonstrated that dual-phase steel associated with the TRIP or "TRIP type multiphase (TMP) steel[2–8)]" which was recently developed has an excellent press formability, except the stretch-flangeability.[5–7)] As the TMP steel possesses high fatigue strength[8)] and high impact absorbed energy,[9)] many researchers tried to apply the steel to the automotive underbody parts[9)] and impact members up to now. However, the poor stretch-flangeability obstructed the underbody applications.

The inferior stretch-flangeability of the TMP steel may be caused by a small void-initiation strain at the ferrite matrix/second phase interface.[6,7)] Generally, the bainitic steel has a good stretch-flangeability due to uniform fine structure or high localized ductility. So, replacing the ferrite matrix with bainitic ferrite lath structure is expected to improve the stretch-flangeability of the TMP steel. Such a steel with the bainitic ferrite plus the retained austenite structure or "TRIP type bainitic (TB) steel" has been already developed as 0.2–0.6mass%C–Si–Mn[10–14)] or C–Si–Ni[10–12)] steels. Also, the characteristics of microstructure and the mechanical properties were reported by some research groups.[9–13)] However, there is no systematic research on the ductility and deformation mechanism of the TB steel from a viewpoint of improving the press formability.

To develop a new high-strength sheet steel with an excellent stretch-flangeability, the effects of austempering conditions on the retained austenite characteristics and the tensile properties, particularly ductility, of the TB steel were examined in the present study. In addition, deformation-transformation behavior and X-ray internal stress of the retained austenite were investigated for characterizing the retained austenite stability and deformation mechanism of the TB steel.

2. Experimental Procedure

Vacuum-melted 30 mm thick slabs with chemical composition of 0.20C, 1.51Si, 1.51Mn, 0.015P, 0.0011S, 0.040Al and 0.0021N (mass%) were used in this study. Martensite-start temperature (M_S) of the steel was estimated to be 417°C using the following equation.[15)]

$$M_S(°C) = 561 - 474 \times C(mass\%) - 33 \times Mn(mass\%) - 17Ni(mass\%) - 17 \times Cr(mass\%) - 21Mo(mass\%) \quad \text{.....(1)}$$

The slabs were cold-rolled to 1.2 mm in thickness after hot-rolling to 3.5 mm in thickness and subsequently were austempered at T_A=350–475°C for 10–10 000 s in salt bath after annealing at 950°C for 1 200 s, as illustrated in **Fig. 1**. For comparison, the TMP steel austempered at 400°C for 1 000 s after intercritical annealing at 780°C for 1 200 s, which possesses the same composition as the TB steel, was also employed in this study.

Tensile test was carried out on an Instron type of tensile testing machine at 20°C and at a crosshead speed of 1 mm/min, using the JIS-13B specimens of 60 mm in length

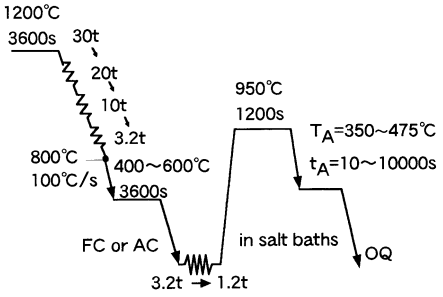

Fig. 1. Hot and cold rolling processing and heat-treatment of TB steel.

Table 1. X-ray measurement conditions and material constants.

Phase	α	γ
X-ray	Cr-K α	
Filter	V	
Voltage, Current	40 kV – 30 mA	
Slit	0.5 deg.	
Irradiation Mask	5×8 mm²	
Scanning Speed	1 deg./min	
ψ	10, 20, 30, 40, 45 deg.	
Diffraction Plane	(211)	(220)
Young's Modulus	223 GPa	192 GPa
Poisson's Ratio	0.28	0.28

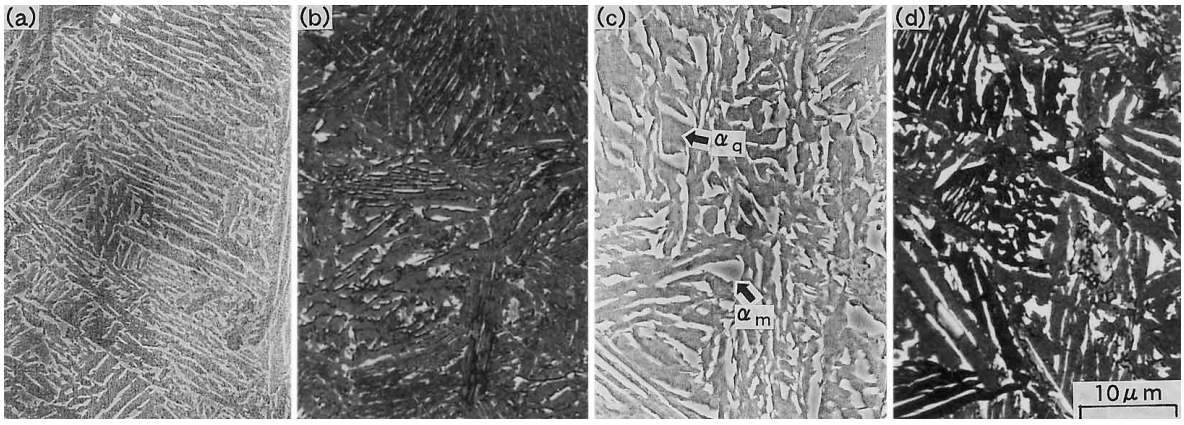

Fig. 2. Microstructure of TB steel austempered at (a, b) 375°C or (c, d) 450°C for 200 s, in which white phase in (b) and (d) represent retained austenite and/or martensite (α_m) and gray phase is bainitic ferrite or quasi-ferrite (α_q). (a) and (c): nital etching, (b) and (d): LePera etching.

(gauge length: 50 mm) by 12.5 mm in width by 1.2 mm in thickness, parallel to the rolling direction. Volume fraction of the retained austenite was quantified on the basis of the integrated intensity of $(200)_\alpha$, $(211)_\alpha$, $(200)_\gamma$, $(220)_\gamma$ and $(311)_\gamma$ diffraction peaks,[16] using Mo-K$_\alpha$ radiation. Initial martensite and bainite phases in as-austempered steel were distinguished from the retained austenite in terms of etching with modified LePera reagent.[17]

Carbon concentration (C_γ, mass%) of the retained austenite was estimated from the following equation and the lattice constant (a_γ, $\times 10^{-10}$ m) which was measured from the $(220)_\gamma$ diffraction peak using Cr-K$_\alpha$ radiation.[3]

$$C_\gamma=(a_\gamma-3.5467)/0.0467 \quad \text{.....(2)}$$

The 2θ–$\sin^2\psi$ method[18] was applied to X-ray studies of internal stress (σ_X). Namely, variations in 2θ with $\sin^2\psi$ were measured with respect to $(220)_\gamma$ diffraction peaks using Cr-K$_\alpha$ radiation. Then, the slope ($d2\theta/d\sin^2\psi$) was substituted in the following equation.

$$\sigma_X=-\{E/2(1+\nu)\}\cot\theta_0(d2\theta/d\sin 2\psi) \quad \text{.....(3)}$$

where θ_0 and θ represent diffraction angles under free strain and on straining, respectively. The term ψ is an angle between reflecting-plane normal and surface normal. The terms E and ν are the Young's modulus and the Poisson's ratio of each phase, respectively. The measurement conditions and material constants in Eq. (2) are shown in **Table 1**.

To clarify deformation–transformation behavior of the retained austenite, thin foils of deformed specimens were observed in a transmission electron microscope. Also, the line breadth at a half-maximum X-ray intensity ($\Delta\theta_X$) which corresponds to plastic strain and dislocation density was measured from the $(220)_\gamma$ diffraction peak using Cr-K$_\alpha$ radiation.

3. Results

3.1. Retained Austenite Characteristics

Figures 2 and **3** show typical micrographs of as-austempered TB steels. From these photographs, it is found that the microstructure of the TB steel mainly consists of bainitic ferrite lath matrix and interlath retained austenite films (Fig. 3). If austempered at temperatures higher than martensite-start temperature of the steel (M_S=417°C), quasi-ferrite[19] and blocky martensite phases coexist with coarsened retained austenite films and bainitic ferrite matrix with the decreased dislocation density.

Figure 4 shows typical microstructure of the TB steels subjected to prolonged austempering time. When austempered at temperatures above M_S, the prolonged austempering increases volume fraction of quasi-ferrite and bainite phases.

Figures 5 and **6** show the variations in initial volume fraction ($f_{\gamma 0}$) and initial carbon concentration ($C_{\gamma 0}$) of retained austenite with austempering time (t_A) and temperature (T_A) in the TB steel, respectively. From these figures, the followings are recognized.

(1) A large amount of retained austenite with high carbon concentration is obtained when austempered at relatively low temperatures for t_A=100–3 000 s.

(2) Under these conditions, the volume fraction of re-

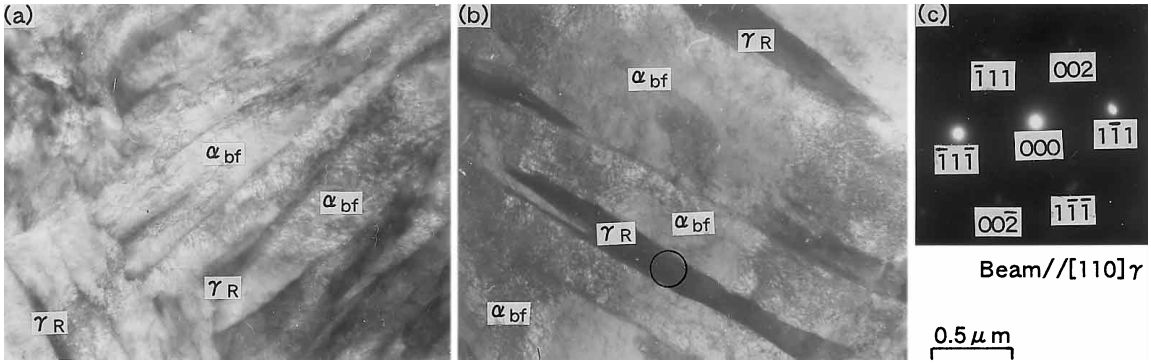

Fig. 3. Transmission electron micrographs of interlath retained austenite films (γ_R) along bainitic ferrite lath structure (α_{bf}) in TB steel austempered at (a) 375°C or (b) 450°C for 200 s; (a) and (b): bright-field image, (c): selected area diffraction pattern of encircled area in (b).

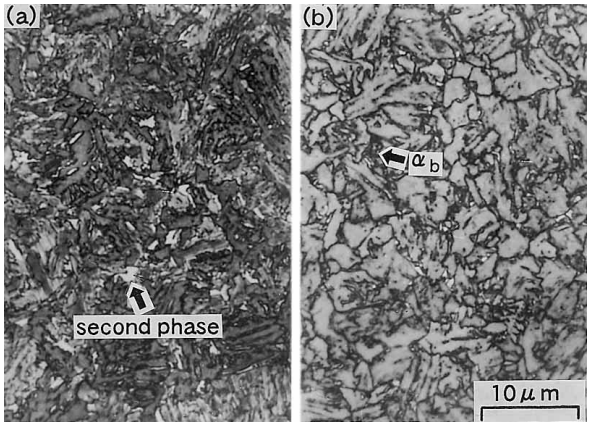

Fig. 4. Optical micrographs of TB steel austempered at (a) 375°C or (b) 450°C for 10 000 s, in which "α_b" represents bainite phase. (LePera etching)

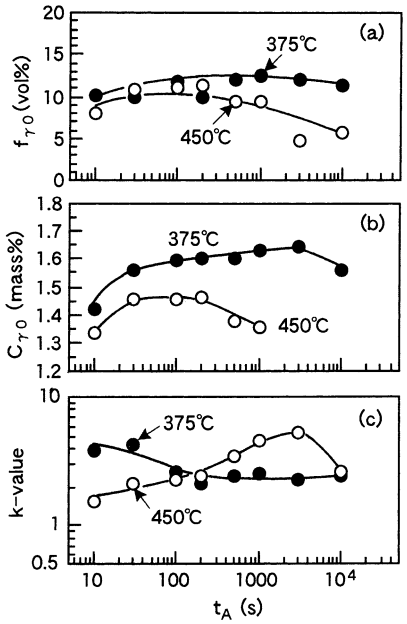

Fig. 5. Variations in (a) initial volume fraction ($f_{\gamma 0}$) and (b) initial carbon concentration ($C_{\gamma 0}$) of retained austenite and (c) k-value with austempering time (t_A) in TB steel austempered at 375°C or 450°C.

tained austenite is between 8 and 12 vol% and its carbon concentration is ranging from 1.44 to 1.65 mass%.

(3) The austempering temperature decides the initial carbon concentration of retained austenite rather than the amount of retained austenite.

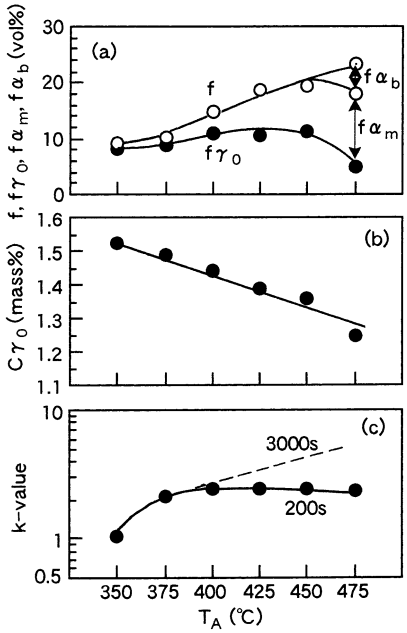

Fig. 6. Variations in (a) initial volume fraction ($f_{\gamma 0}$) and (b) carbon concentration ($C_{\gamma 0}$) of retained austenite and (c) k-value with austempering temperature (T_A) in TB steel, in which f, f_{α_m} and f_{α_b} represent volume fractions of second phase, initial martensite and bainite, respectively. (t_A=200 s)

Retained austenite stability against the strain-induced martensite transformation or k-value[2,3] which is defined as the following equation is shown in Figs. 5(c) and 6(c).

$$\log f_\gamma = \log f_{\gamma 0} - k\varepsilon_P \quad \text{.....(4)}$$

where ε_P is a plastic strain. From these figures, it is found that the k-value is controlled by both the austempering time and temperature.

3.2. Tensile Properties

Figures 7 and **8** show the effects of austempering time and austempering temperature on tensile properties, respectively. The TB steels have 0.2 % offset proof stress or yield stress (*YS*) more than 500 MPa and tensile strength (*TS*) more than 850 MPa. Large uniform and total elongations (*UEl* and *TEl*) are obtained when the steels were austem-

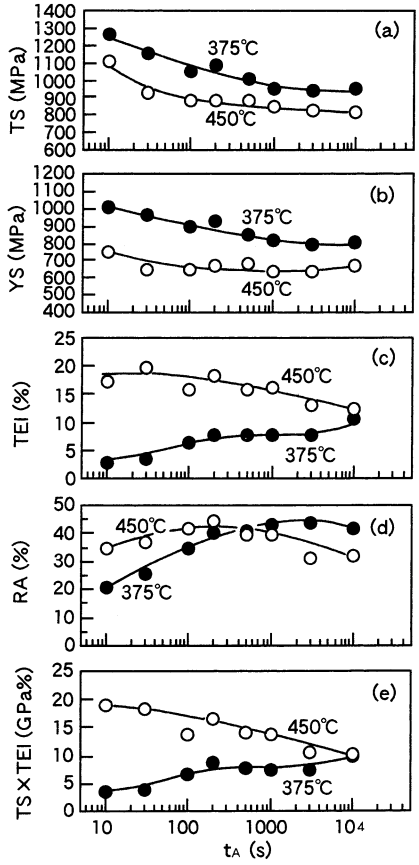

Fig. 7. Variations in tensile properties with austempering time (t_A) in TB steel austempered at 375°C or 450°C.
YS: 0.2% offset proof stress or yield stress, *TS*: tensile strength, *TEl*: total elongation, *RA*: reduction of area, *TS*×*TEl*: strength-ductility balance

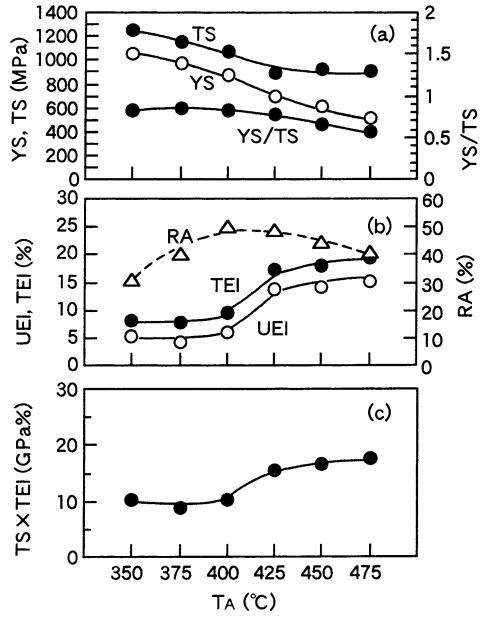

Fig. 8. Variations in tensile properties with austempering temperature (T_A) in TB steel. (t_A=200s)
YS: 0.2% offset proof stress or yield stress, TS: tensile strength, *YS*/*TS*: yield ratio, *UEl*: uniform elongation, *TEl*: total elongation, *RA*: reduction of area, *TS*×*TEl*: strength-ductility balance

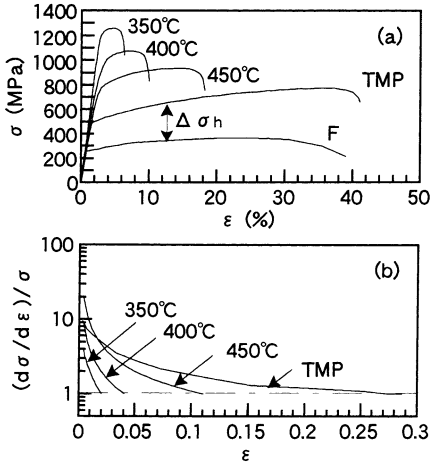

Fig. 9. Changes in flow stress (σ) and ($d\sigma/d\varepsilon$)/σ ($d\sigma/d\varepsilon$: strain-hardening rate) with austempering temperature in TB steel, in which "F" represents flow curve of 0.006C–1.50Si–1.50Mn–0.036Al (mass%) ferritic steel.

pered at T_A=425–475°C for 10–1 000 s. The resultant strength–ductility balance (*TS*×*TEl*) is larger than those of other high strength steels such as the ferrite-martensite dual-phase steel (*TS*=900 MPa, *TS*×*TEl*=11.6 GPa%) and the bainitic steel (*TS*=650 MPa, *TS*×*TEl*=8.0 GPa%),[5] except that of the TMP steel (*TS*=800 MPa, *TS*×*TEl*=25–30 GPa%).

It is noteworthy that the TB steels austempered at temperatures lower than M_S possess a relatively large reduction of area (*RA*), despite small uniform and total elongations. In addition, the prolonged austempering time enhances the reduction of area, as shown in Fig. 7(d).

Figure 9 shows typical flow curves and strain-hardening behavior of the TB steels austempered at various temperatures. When the TB steels were austempered at temperatures above M_S, these flow curves are chracterized by continuous yielding and small strain hardening, in the similar way as the TMP steel. Even if deformed to maximum load, no void initiates at the matrix/second phase interface in the TB steels. This behavior is considerably different from that of TMP steel in which many voids occur before maximum load.

3.3. Deformation–Transformation Behavior of Retained Austenite Films

For investigating deformation mechanism of the TB steel, deformation-transformation behavior and a long-range internal stress of the retained austenite films during tensile deformation were examined in the TB steel austempered at 450°C for 200 s which possessed good ductility (Figs. 7 and 8).

Figure 10 shows transmission electron micrographs of the TB steel strained to 10% in tension. From the photographs, it is observed that a part of original retained austenites transforms to twinned martensite. However, no deformation twin is recognized in the retained austenite, differing from cases of high carbon bainitic steel[14] and TMP steel.[2]

Figures 11 and **12**(a) show the variations in untransformed retained austenite content (f_γ), the ratio of line breadth at a half maximum X-ray intensity of strained

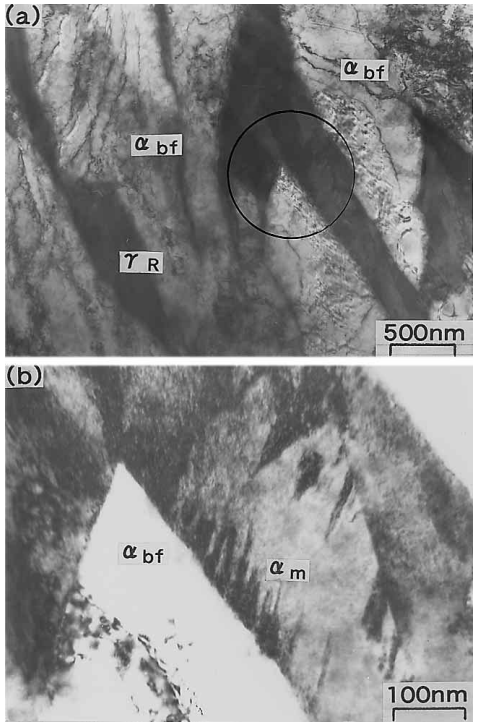

Fig. 10. Transmission electron micrographs showing strain-induced twin martensite (α_m) in original retained austenite of TB steel austempered at 450°C for 200 s. (b) corresponds to encircled region of (a).

austenite to that of unstrained one ($\Delta\theta_{X\gamma}/\Delta\theta_{X\gamma 0}$) and X-ray internal stress in the retained austenite ($\sigma_{X\gamma}$) during deformation for the TB and TMP steels (f=0.261, $f_{\gamma 0}$=0.190, $C_{\gamma 0}$=1.38 mass%). From these figures, it is found that retained austenite stability against the strain-induced transformation is nearly equal to that of the TMP steel, and the untransformed retained austenite strain-hardens much more than that of the TMP steel. In addition, a high long-range tensile internal stress of about 300 MPa which is somewhat higher than that of the TMP steel takes place in the retained austenite of the TB steel.

4. Discussion

4.1. Retained Austenite Stability

Takahashi and Bhadeshia[20] have proposed for carbide-free bainitic steels that carbon concentration of retained austenite is equal to that in austenite at T_0 temperature where austenite and ferrite with the same chemical composition have identical free energies. According to their theory, the carbon concentration at the T_0 increases with decreasing austempering temperature, before diffusionless transformation becomes impossible.

Figure 13 shows measured carbon concentration of retained austenite in the TB steel plotted in Fe–1.5Si–1.5Mn–C system equilibrium which was computed by THERMO-CALC. In the figure, the measured carbon concentration appears to vary along T_0 temperature/carbon concentration line, although it is larger than the calculated one. So, high initial carbon concentration of the retained austenite in the TB steels austempered at lower temperatures (Fig. 6(b)) may result from high carbon concentration at the T_0. Also, the measured carbon concentration of retained austenite in the TB steel is found to be somewhat higher than that of the TMP steel. This is considered to be caused by the absence of bainite islands which can consume the solute carbon as cementites.

Generally, high carbon concentration of retained austen-

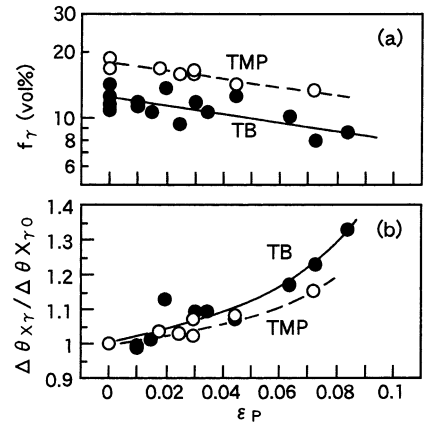

Fig. 11. Variations in (a) retained austenite content (f_γ) and (b) ratio of line breadth at a half-maximum X-ray intensity ($\Delta\theta_{X\gamma}/\Delta\theta_{X\gamma 0}$) with plastic strain ($\varepsilon_P$) in TB steel austempered at 450°C for 200 s.

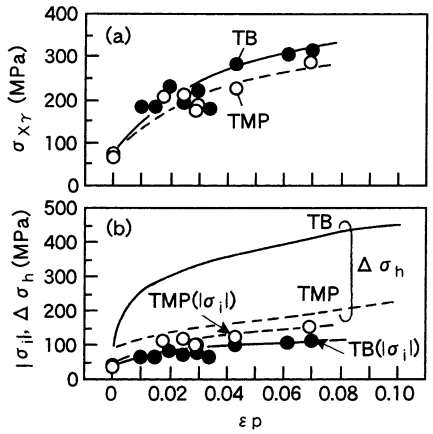

Fig. 12. Variations in (a) X-ray internal stress ($\sigma_{X\gamma}$) and (b) absolute calculated internal stress in matrix ($|\sigma_i|$) and total hardening increament ($\Delta\sigma_h$) with plastic strain (ε_P) in TB steel austempered at 450°C for 200 s.

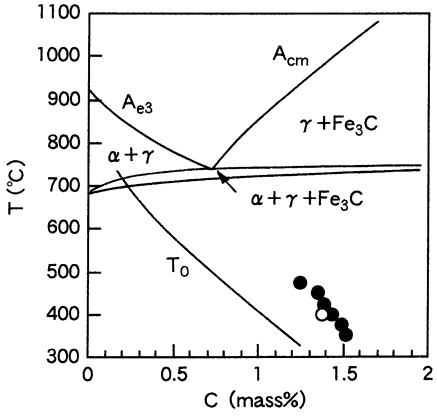

Fig. 13. Equilibrium diagram of Fe–(1.5Si–1.5Mn)–C system computed by THERMO-CALC, in which marks represent measured carbon concentrations of retained austenite of TB (●) and TMP (○) steels.

ite increases its stability against the strain-induced transformation or decreases the *k*-value.[2,3] However, the *k*-values of the TB steels austempered at 400–475°C were nearly constant, despite different carbon concentration of retained austenite (Fig. 6(c)). From Fig. 5(c), the *k*-value is found to be increased by the prolonged austempering for the TB steel austempered at 450°C. Therefore, it is supposed that the *k*-value essentially reduces with decreasing austempering temperature or with increasing carbon concentration of retained austenite, as dotted line in Fig. 6(c).

When the TB and TMP steels with the same chemistry were austempered at the same temperature (400°C), carbon concentration of retained austenite ($C_{\gamma 0}$=1.45 mass%) in the TB steel was higher than that ($C_{\gamma 0}$=1.38 mass%) in the TMP steel (Fig. 13). However, the *k*-value of the TB steel was nearly equal to that (*k*=2.5) of the TMP steel. This is because higher flow stress and smaller difference in flow stress between the matrix and retained austenite films (resulting in a larger plastic strain in the retained austenite) in the TB steel promotes the strain-induced martensite transformation of the retained austenite.[21]

4.2. Role of Retained Austenite on Strain-hardening

The TB steel austempered at 450°C was composed of two phases, namely bainitic ferrite matrix and second phase (interlath retained austenite film plus blocky martensite), as shown in Fig. 2 (c, d). Hence, the deformation is expected to be controlled by the following two items,[22] in the similar way as the TMP steel.

(i) compressive long range internal stress in the matrix which was resulted from untransformed retained austenite and other hard second phases.
(ii) strain-induced transformation of the retained austenite which results in martensite hardening and stress relaxation (or plastic relaxation).

The item (i) contributes to large strain-hardening at an early stage. On the other hand, the item (ii) brings on a relatively high strain-hardening rate in a large strain range and consequently suppresses the onset of diffuse necking. The strain-induced transformation simultaneously relaxes the localized stress concentration at the matrix/second phase interface to suppress the void-initiation.

According to the continuum model[22–25] associated with Eshelby's theory,[26] when the TMP steel is plastically strained to a given strain ε in uniaxial tension, a true increment of strain hardening $\Delta\sigma_h$, as illustrated in Fig. 9(a), is obtained from the following equation.

$$\Delta\sigma_h(\varepsilon)=\sigma(\varepsilon)-\sigma^M(\varepsilon)$$
$$=\sigma_i(\varepsilon)+\sigma_f(\varepsilon)+\sigma_t(\varepsilon) \quad \text{.....(5)}$$

where σ and σ^M represent flow stresses of the TMP steel and soft ferrite matrix, respectively. And, the σ_i, the σ_f and the σ_t are "the mean internal stress",[24] "the forest hardening"[27] and "the strain-induced martensite hardening",[22] respectively. And, they are given as follows:

$$\sigma_i(\varepsilon)=\{(7-5\nu)\mu/5(1-\nu)\}f\varepsilon_p^u$$
$$=-3/2(f/(1-f))\sigma_{X\gamma}(\varepsilon) \quad \text{.....(6)}$$

$$\sigma_f(\varepsilon)=\zeta\mu(\mathbf{b}f\varepsilon/2r)^{1/2} \quad \text{.....(7)}$$

$$\sigma_t(\varepsilon)=\xi f^*_{\alpha_m} \quad \text{.....(8)}$$

where μ and ν are the shear modulus and the Poisson's ratio of each phase, respectively. The terms ζ and ξ are constant. The *f* and the $f^*_{\alpha_m}$ are the volume fractions of second phase and strain-induced martensite, respectively. The ε_p^u is unrelaxed strain[25] (stress free strain[26]), the **b** is the dimension of the Burgers vector, and the *r* denotes the mean diameter of the second phase particles.

If the preceding continuum theory is applied to the deformation of the TB steel, the $|\sigma_i|$ and $|\sigma_i|/\Delta\sigma_h$ are calculated from Eqs. (5) and (6), as shown in Fig. 12(b). In this calculation, the flow stress of a 0.006C–1.50Si–1.50Mn, mass%, ferritic steel[28] ("F" in Fig. 9(a)) which was modified the grain size by the Hall–Petch equation was used for the σ^M of the TMP steel. And, the bainitic ferrite matrix of the TB steel was assumed to possess a yield stress of 450 MPa[29] and the same strain-hardening rate as the above ferritc steel. In addition, *f*=0.193 (TB steel) and *f*=0.261 (TMP steel) were substituted into Eq. (6). From Fig. 12(b), the followings are obvious.

Compressive mean internal stress of around 100 MPa is developed in the matrix of the TB steel, which is lower than that of the TDP steel. The $|\sigma_i|/\Delta\sigma_h$ ranges from 0.2 to 0.3, in contrast to $|\sigma_i|/\Delta\sigma_h$=0.5–0.8 in a case of the TMP steel. Thus, in the TB steel a contribution of the item (i) to the strain-hardening rate is concluded to be smaller than that of the item (ii), differing with the case of the TMP steel.

4.3. Deformation Mechnism of TB Steel

The TB steel possessed smaller total elongation than the TMP steel, as shown in Fig. 9, although the volume fraction and stability of retained austenite are equivalent to those of the TMP steel. This may be explained as follows.

According to the previous study,[22] large total elongation of the TMP steel was ascribed with high internal stress hardening over all strain range and large strain-induced martensite hardening in a large strain range, despite easy void initiation at the matrix/second phase interface in a strain range of 10–15 %. The contribution of compressive internal stress hardening to total strain-hardening in the TB steel was smaller than that of the TMP steel (Fig. 12(b)). This is considered to lower the strain-hardening rate in an early stage, even if the hardening due to initial martensite and the strain-induced martensite hardening are employed to enhance the strain-hardening rate in an early stage and in a large strain range, respectively. Consequently, the diffuse necking occurs in a realtively small strain range.

The above mentioned idea suggests that both the initial martensite hardening of a large amount of original martensite and the TRIP effect of retained austenite (*i.e.*, stress relaxation and strain-induced martensite hardening) play an important role in enhancing total elongation of the TB steel. Also, the suppressed void formation is considered to contribute to the large total elongation. When austempered at temperatures below M_S, the TB steel exhibited only a small total elongation due to rapid fall of strain-hardening rate (Fig. 9(b)). This may be caused by (i) small internal stress hardening and initial martensite hardening resulting from a small volume fraction of second phase (Fig. 6(a)) and (ii) bainitic ferrite matrix with high initial dislocation density (Fig. 3 (a)).

5. Conclusions

(1) The TB steel consisted of bainitic ferrite lath matrix and stable retained austenite films of 5–12 vol% whose carbon concentration was linearly increased with decreasing austempering temperature. However, a large amount of initial blocky martensite coexisted with these phases when austempered at temperatures above M_S.

(2) When compared with the TMP steel austempered at the same temperature, the retained austenite stability against the strain-induced transformation was nearly equal to that of the TMP steel, despite high carbon concentration and thin morphology.

(3) The TB steels austempered at temperatures above M_S completed larger total elongation and reduction of area than other high-strength steels, except the TMP steel.

(4) In the TB steel, untransformed retained austenite as a hard phase brought on the compressive internal stress in the matrix, but the contribution to the strain-hardening was very smaller than that of the TMP steel.

(5) The large total elongation of the TB steel was concluded to be caused by the TRIP effect of retained austenite (stress relaxation and strain-induced martensite hardening) and initial martensite hardening, as well as the forest hardening.

REFERENCES

1) V. F. Zackay, E. R. Parker, D. Fahr and R. Bush: *Trans. Am. Soc. Met*., **60** (1967), 252.
2) K. Sugimoto, M. Kobayashi and S. Hashimoto: *Metall. Trans*., **23A** (1992), 3085.
3) K. Sugimoto, N. Usui, M. Kobayashi and S. Hashimoto: *ISIJ Int*., **32** (1992), 1311.
4) K. Sugimoto, M. Kobayashi, S. Yasuki and S. Hashimoto: *Mater. Trans. JIM*, **36** (1995), 632.
5) K. Sugimoto, A. Nagasaka, M. Kobayashi and S. Hashimoto: *ISIJ Int*., **35** (1995), 1407.
6) Y. Hirose, S. Nakai, H. Fukuyama, S. Sudoh and K. Ueno: *J. Jpn. Soc. Technol. Plast*., **35** (1994), 1071.
7) S. Hiwatashi, M. Takahashi, T. Katayama and M. Usuda: *J. Jpn. Soc. Technol. Plast*., **35** (1994), 1109.
8) K. Sugimoto, X. Sun, M. Kobayashi, T. Haga and H. Shirasawa: *Trans. Jpn. Soc. Mech. Eng*., **60A** (1997), 717.
9) Y. Ojima, Y. Shiroi, Y. Taniguchi and K. Kato: *SAE Tech. Paper Series*, **980954**, (1998), 39.
10) H. K. D. H. Bhadeshia and D. V. Edmonds: *Met. Sci*., **17** (1983), 411.
11) H. K. D. H. Bhadeshia and D. V. Edmonds: *Met. Sci*., **17** (1983), 420.
12) V. T. T. Miihkinen and D. V. Edmonds: *Mater. Sci. Technol*., **3** (1987), 422.
13) K. Tsuzaki, A. Kodai and T. Maki: *Metall. Mater. Trans. A*, **25A** (1994), 2009.
14) K. Shinoda and T. Yamada: *J. Jpn. Soc. Heat Treat*., **20** (1980), 326.
15) W. Steven and A. G. Haynes: *J. Iron Steel Inst*., **183** (1956), 349.
16) H. Maruyama: *J. Jpn. Soc. Heat Treat*., **17** (1977), 198.
17) S. Bandoh, O. Matsumura and Y. Sakuma: *Trans. Iron Steel Inst. Jpn*., **28** (1988), 569.
18) Soc. Mat. Sci. Jpn., Standard Measurement Method of X-Ray Stress, (1977).
19) K. Amano and T. Araki: Atlas for Bainitic Microstructures, Vol. 1, ISIJ Tokyo, (1992), 21.
20) M. Takahashi and H. K. D. Bhadeshia: *Mater. Trans. JIM*, **32** (1991), 689.
21) S. V. Radcliffe and M. Schatz: *Acta Metall*., **10** (1962), 201.
22) K. Sugimoto, M. Kobayashi and S. Yasuki: *Metall. Mater. Trans. A*, **28A** (1997), 2637.
23) Y. W. Chang and R. J. Asaro: *Met. Sci*., **12** (1978), 277.
24) Y. Tomota and I. Tamura: *Tetsu-to-Hagané*, **68** (1982), 1147.
25) T. Mura and T. Mori: Micromechanics, Baifu-kan, Tokyo, (1976).
26) J. D. Eshelby: *Proc. R. Soc*., *Ser. A*, **A241** (1957), 376.
27) M. F. Ashby: *Philos. Mag.*, **14** (1966), 1157.
28) K. Sugimoto, M. Kobayashi, H. Matsushima and S. Hashimoto: *Trans. Jpn. Soc. Mech. Eng*., **61A** (1995), 80.
29) R. W. K. Honeycombe and F. B. Pickering: *Metall. Trans*., **3** (1972), 1099.